



Passive Treatment of Circumneutral Mine Drainage from the St. Louis Mine Tunnel, Rico CO: Part 2—Vertical Biotreatment Train Pilot Study

Daniel M. Dean¹ · James R. Fricke¹ · Arthur C. Riese² · Terry J. Moore³ · Anthony R. Brown³

Received: 28 December 2020 / Accepted: 15 February 2022 / Published online: 3 May 2022
© The Author(s) 2022

Abstract

This is the second of three papers dealing with metal-bearing circumneutral mine drainage from the inactive Rico-Argentine mine site located at an elevation of ≈ 2740 m (9000 feet) in the San Juan mountain range in southwestern Colorado. This paper evaluates two years of mine drainage treatment using a passive system that included a vertical-flow engineered biotreatment cell. The collapsed St. Louis Tunnel (SLT) discharges circumneutral mine water from several sources that contains elevated concentrations of Cd, Cu, Fe, Mn, Zn. A demonstration-scale 114 L/min (30 gpm) gravity-flow passive treatment system was installed, consisting of a settling basin (utilizing coagulant addition to improve suspended solids settling efficiency), an anaerobic sulfate-reducing bioreactor, and an aeration cascade for effluent polishing. The treatment system generally met target treatment goals for Cd, Cu, Fe, and Pb. Nanophase ZnS in system effluent decreased the frequency of meeting total Zn project treatment goals. Unexpectedly high levels of Mn removal were observed in both the anaerobic bioreactor and the aeration cascade. Large seasonal variations in influent metals concentrations and pH present the greatest challenge in managing system performance.

Keywords SRB · Sulfide · Cadmium · Copper · Iron · Manganese · Zinc · Metals · High elevation · Colorado · Seasonal · Telemetry · Constructed wetlands

Introduction

At the remote inactive Rico-Argentine silver–lead–zinc mine site located in southwestern Colorado, metal-bearing mine drainage from several sources discharges year-round from a collapsed former haulage and drainage tunnel known as the Saint Louis Tunnel (SLT). Discharge from the SLT is circumneutral and contains elevated concentrations of Cd, Cu, Fe, Mn, and Zn. Flow rates range from 1670 L/min (440 gpm) to 5320 L/min (1400 gpm) (details in Lewis-Russ et al. 2022). The site is located at an elevation of ≈ 2743 m (9000 ft) in the San Juan mountain range. Winter weather conditions at the site are typical for high-elevation

alpine environments; temperatures regularly reach as low as -29 °C (-20 °F), average annual snowfall is 4390 mm (173 in), and multiple avalanche paths runout on the site. Additional background information about the site can be found in Lewis-Russ et al. (2022).

Because of the site's remote location, high elevation, periodic avalanches, and extreme winter weather, year-round operation of active chemical treatment systems, such as lime treatment, is operationally difficult. The site was considered an excellent candidate for a gravity-flow passive treatment system that would require minimal operation and monitoring during the winter season. Bench- and pilot-scale studies were started in 2012 (Sobolewski et al. 2022) and indicated that the mine drainage at the site was amenable to passive treatment via augmented gravity settling and sulfate-reducing bioreactors. The primary objectives of this study were to determine achievable year-round project-specific treatment levels, to understand seasonal management requirements for year-round operation, and to develop design criteria for a potential full-scale treatment system.

This paper is the second of three related papers regarding this project. The first, Lewis-Russ et al. (2022), presents site

✉ Terry J. Moore
terry.moore.texas@gmail.com

¹ Resource Environmental Consultants Inc, 8496 Harrison St., Suite 102, Midvale, UT 84047, USA

² EnSci Inc, 1501 East Quincy Ave, Cherry Hills Village, CO 80113, USA

³ Atlantic Richfield Company, 201 Helios Way, Houston, TX 77079, USA

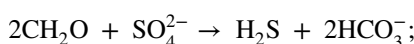
historic data and a conceptual site model for the seasonal SLT flow and composition. This paper presents design and performance information and lessons learned from a passive vertical-flow system. The third paper, Sobolewski et al. (2022), presents information from a passive horizontal-flow system. Studies of the two treatment systems were conducted over the same time period, using the same seasonally varying influent water, at a nominal 30 gpm flow rate to facilitate evaluation of the technologies that would be further tested at the site.

Background

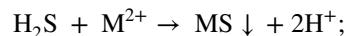
Passive treatment of metal-bearing mine drainage is well-documented in the literature. As early as the late 1970s, papers were published describing natural attenuation of acidic mine drainage (AMD) that passed through naturally occurring *Sphagnum* bogs in Ohio (Huntsman et al. 1978) and West Virginia (Wieder and Lang 1982). Following these discoveries and passage of the Clean Water Act (CWA) in the United States in 1972, the potential for low-cost treatment of metals-bearing mine drainage using wetland-type treatment systems generated considerable academic and regulatory interest. By the early 1990s, overview papers summarizing the technology had been presented and published (e.g. Hedin et al. 1994; Kleinmann 1991; Nairn and Hedin 1993). Full-scale sulfate-reducing bioreactors treating flows in excess of 3785 L/min (1000 gpm) were in use by the late 1990s (Gusek et al. 1998).

Implementation of passive treatment in general, and sulfate-reducing bioreactors specifically, slowed in the early to mid-2000s following poor performance or outright failure of several prominent systems (Johnson and Hallberg 2002). The most common failure modes were loss of hydraulic conductivity in the organic matrix due to insufficient pre-treatment of influent suspended solids, selection of overly fine-grained matrix materials, and selection of matrix materials with poorly bioavailable organic carbon (Neculita et al. 2007). Subsequent research attempted to identify and devise matrix materials that optimize organic carbon bioavailability (Figueroa et al. 2004) and provide grain sizes that ensure long-term maintenance of hydraulic conductivity (Hagerty et al. 2011).

Sulfate-reducing bacteria (SRB) are obligate anaerobes capable of reducing sulfate to sulfide when provided with a labile organic carbon source and an anaerobic environment. Organic carbon serves as the electron donor while sulfate serves as the terminal electron acceptor. The reaction is generally expressed as:



where CH_2O in the sulfate reduction reaction is a generic representation of simple organic carbon (Widdel 1988). The soluble sulfides (H_2S , HS^-) react with metals to form insoluble metal sulfide precipitates:



where M is typically a divalent cationic metal such as Cd, Fe, Ni, Cu, or Zn. Sulfate-reducing bacteria are only capable of oxidizing simple, short-chain organic carbon compounds and cannot directly utilize complex organic carbon sources (i.e. cellulose, hemicellulose) provided in typical sulfate-reducing bioreactors (Postgate 1984). The SRB in these bioreactors rely on other cellulolytic and fermenter microbes to degrade complex organic carbon compounds into simpler molecules, and SRB activity can be limited by the activity of these cellulose-degrading microflora (Figueroa et al. 2004; Neculita et al. 2007).

Using thermodynamic modelling to explain metal concentrations from wetlands systems has had limited success, due to limited availability of thermodynamic data for poorly crystalline sulfide mineral phases and difficulties in filtering colloidal metal sulfide particles from water samples (Gammons and Frandsen 2001). Use of total and dissolved metal data is important in understanding metal partitioning in wetland systems (Gammons et al. 2000).

Methods and Materials

A general arrangement drawing of the passive treatment system, herein referred to as the vertical biotreatment train (VBTT) is presented in Fig. 1. The principal components of the VBTT consist of a settling basin (settling basin no. 2 [SB2]) for removal of settleable solids (primarily particulate Fe oxyhydroxides with other sorbed metals), an anaerobic sulfate-reducing bioreactor (biocell) for removal of Cd, Cu, and Zn via sulfide precipitation, and an aeration cascade for removal of residual dissolved sulfide and restoration of dissolved oxygen (DO).

Settling Basin No. 2 (SB2)

SB2 was constructed as a gravity-fed, geomembrane-lined basin with a surface area of 191 m², a volume of 141 m³, a nominal hydraulic residence time (HRT) of 20 h at a flow rate of 114 L/min (30 gpm), and a hydraulic loading rate of 0.60 L/min/m² (0.015 gpm/ft²). SB2 was designed with a long and narrow profile (length to width ratio of 3.4:1) meant to prevent short-circuiting and maximize settling capacity (key SB2 dimensions are presented in supplemental Table S-1). SB2 was designed with a central “sump” area to concentrate settled solids in the deepest part of the basin where they are

isolated from disturbance by wave action and can be more easily removed during maintenance activities. Floating high-density polyethylene (HDPE) insulating balls were placed across the entire surface of SB2 to minimize heat loss during winter operation and reduce wave action at the SB2 water surface. A baffle curtain was installed across the width of SB2 to enhance particle settling by promoting an even distribution of water flow across the basin and reducing short-circuiting. The baffle curtain was installed near the basin inlet to maximize its effect on solids settling.

Unpublished data from a previous pond system at the site indicated that particulate settling rates of raw mine water were too slow to achieve sufficient clarification to prevent plugging of the bioreactor media. These observations were further supported by laboratory particle size analysis, which indicated that 90% of particulates were colloidal in size and finer than 1.24 μm . Laboratory screening was performed to test the efficacy of multiple coagulants and flocculants. Aluminum chlorohydrate was the most effective coagulant tested, practical to implement, and therefore selected for use in this study at a rate of 15 mg/L. The coagulant was added using a peristaltic pump and static mixing chamber just prior to the settling basin.

Biotreatment Cell

The biocell was constructed as a gravity-fed, geomembrane-lined basin with a surface area of 278 m^2 , an organic substrate volume of 272 m^3 , and a nominal HRT of 12 h. Key biocell dimensions, volumes, and estimated matrix porosity are presented in supplemental Table S-2. The organic matrix consisted of $\approx 65\%$ (by volume) wood chips (2.5 cm [1.0 inch] to 5 cm [2.0 inch] diameter), 25% wood shavings (1.3 cm [0.5 inch] to 2.5 cm [1.0 inch] diameter), 5% chopped alfalfa hay, and 5% composted cattle manure. Wood species consisted of pine, fir, spruce, and/or aspen, with primary consideration given to local availability. All wood products had been stockpiled by the vendor for at least 1 year and were not produced from fresh-cut wood.

An influent pipe network consisting of perforated PVC pipe laterals distribute flow across the cell surface. Effluent from the biocell was collected through a network of perforated PVC pipe laterals placed across the entire cell bottom. Effluent laterals are bedded in a layer of drainage rock. The effluent piping was connected to an adjustable-height outlet structure (AgridrainTM) that allows for up to 60 cm (2 ft) of water level adjustment. Water level adjustment provide for HRT control, in order to maintain effluent sulfide concentrations in the optimum range.

Aeration Cascade

The aeration cascade was constructed as a series of five high-density polyethylene (HDPE) troughs, each 0.6 m (2

ft) deep, 0.6 m (2 ft) wide, and 3 m (10 ft) long. Treated effluent free-fall 0.5 m (1.5 ft) between each trough into open water to maximize air-stripping of H_2S gas and O_2 dissolution. Complete design criteria for the aeration cascade are provided in supplemental Table S-3.

Flow through the aeration cascade was entirely gravity-driven and effluent depth was controlled by the spillway elevation of each trough. The number of troughs was selected based on the existing topography. Total hydraulic head loss through the aeration cascade was ≈ 2.3 m (7.5 ft), or $\approx 70\%$ of the 3.2 m (10.5 ft) of head loss through the entire system. This total fall height was within standard criteria for cascade aerators, which typically range from 2 m (6.5 ft) to 7 m (23 ft) (TU Delft 2010). Trough depth and the 0.5 m (1.5 ft) fall height between troughs was selected based on established design criteria for cascade aerators (TU Delft 2010) to maximize aeration efficiency. The downgradient half of each aeration cascade trough was filled with 7.6 cm (3-inch) nominal diameter, angular limestone rock to provide surface area for the growth of aerobic sulfide-oxidizing bacteria. Biological oxidation of sulfide proceeds up to five orders of magnitude more rapidly than abiotic oxidation of sulfide, with the highest rates of biological sulfide oxidation achieved by aerobic chemotrophic bacteria (Luther et al. 2011).

Telemetry System and Analytical Monitoring

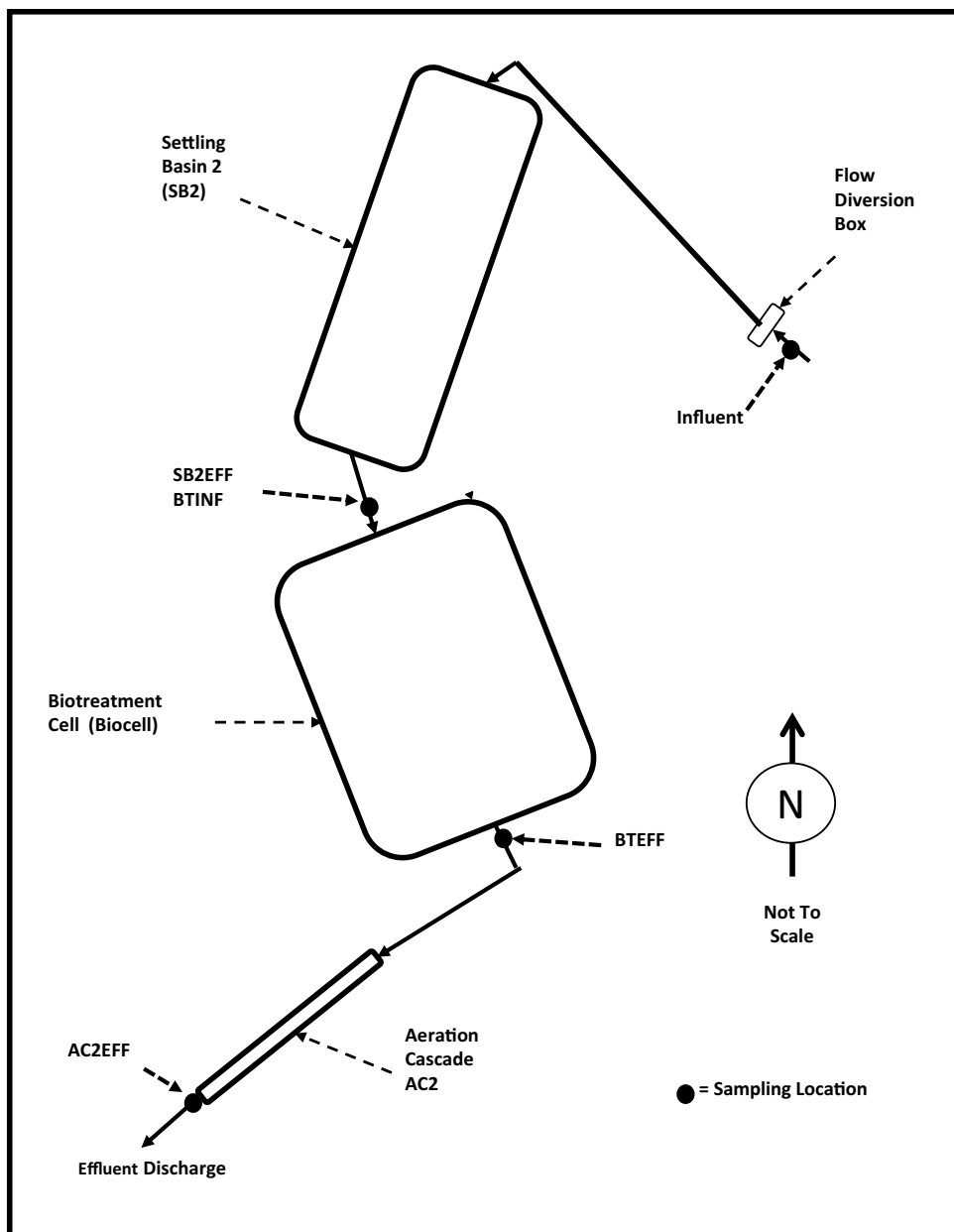
A telemetry system was developed to remotely monitor the status of the VBTT and provide authorized real-time access to data via the internet. Real-time system monitoring minimized the need for personnel to enter the site during winter operations.

The YSI EXO2 sondes were deemed to be most appropriate for long-term deployment in these aquatic environments. They were equipped with several sensors to measure pH, oxidation-reduction potential (ORP), DO, temperature, conductivity, turbidity, and water depth. These sondes were calibrated monthly and periodically cleaned of accumulated biofilm. A weather station and remote cameras were also connected to the telemetry system. Monitors were installed around the aeration cascade to quantify any potential safety risks posed by hydrogen sulfide gas.

Sampling and Analysis

Water samples were collected on a nominal frequency of monthly or semi-monthly from the inlets and/or outlets of each VBTT component (Fig. 1). Sampling frequency was increased to weekly during startup due to rapidly changing conditions. Some sampling events were skipped due to weather and site access issues. Metals analyses were conducted using total and dissolved (filtered using 0.45 μm

Fig. 1 Vertical biotreatment train general arrangement drawing. Includes primary sampling locations, Influent, SB2EFF, BTEFF, and AC2EFF



filters) sample collection techniques (U.S. EPA 1994). Water samples were analyzed for metals and other water quality parameters by a commercial laboratory using standard U.S. EPA-approved methods (Lewis-Russ et al. 2022).

Results

General Water Chemistry

The primary effects on general water chemistry were from the seasonal variability of the influent waters and chemical reduction in the biotreatment cells. Median values for the SLT are included in Table 1 and the seasonal variability

of water chemistry is detailed in Lewis-Russ et al. (2022). The SLT mine water is typically circumneutral; however, the freshet that occurs following snow melt can have pH values (Fig. 2) as low as 6.2 at the initiation of the freshet. The 2015 freshet lasted longest and produced the most negative impact on the biocell, with a minimum pH value of 6.5. Alkalinities ranged from 30 to 150 mg CaCO₃/L.

Start up and maturity of the VBTT was best visualized with biocell effluent sulfide concentration data. Early sample results showed that sulfides were only present in the biocell and aeration cascade effluents and monthly measurements were collected at those locations (Fig. 3). Startup of the system was subject to very low redox values beginning at < -444 mV (vs. Ag/AgCl) and water levels in the

biocell were lowered via the effluent Agridrain to decrease the retention time. Sulfide concentrations increased over the first month to values of 100–1000 mg/L. The readily available organic matter in the biocell medium produced a brown color in the effluent water during this time, as the dissolved organics were degraded. An abrupt decrease in sulfide concentrations from the biocell effluent occurred in November 2014 to values of 4–8 mg/L with a slight downward concentration trend. The onset of the 2015 freshet caused a decrease in sulfides at the BTEFF and AC2EFF locations, reaching <DL values halfway through the freshet season and extending one month past the freshet. Sulfide concentrations at BTEFF increased to an average of 1 mg/L after the 2015 freshet, then decreased less dramatically during the 2016 freshet. Sulfides again recovered to pre-freshet concentrations after the 2016 freshet. Sulfide concentrations in the aeration cascade effluent (AC2EFF) showed a decreasing trend over the duration of the study (especially during 2016) with a final removal efficiency of 97%.

One question at the beginning of the study was whether the harsh winters and low winter temperatures at this elevation would cause a significant seasonal limitation to passive biotreatment. Average monthly temperatures are plotted for each VBTT component effluent (Fig. 4). The geothermally-influenced influent water had a narrow range of 18.3–19.3 °C over the study. Use of insulating balls on the exposed water surface in the settling pond (SB2) limited thermal losses but most thermal loss occurred in the settling basin. The minimum effluent water temperatures emanating from the VBTT were 8 °C in November 2015 (AC2EFF). Year-round input of warm geothermal water into the system resulted in minimal seasonal thermal effects on treatment efficiency that were otherwise overwhelmed by the seasonal influent water chemistry effects of the annual freshet.

Metals Concentrations

The greatest factor influencing metals concentrations discharged from the VBTT was the seasonal influent metals concentrations and flows, as described in Lewis-Russ et al. (2022). These variations are attributable to snowmelt infiltration into the mine workings and dissolution of soluble metal salts and acids. Influent concentrations of total Cd, Cu, Mn, and Zn increased by an average of 330%, 560%, 111% and 396% in spring 2015 and 2016 (Table 2). Time series plots for Cd, Cu, Fe, Mn, Pb, and Zn total concentrations are contained in Figs. 5, 6, 7, 8, 9, 10, respectively, for the VBTT influent and effluents from the SB2 (SB2EFF), the biocell (BTEFF), and aeration cascade (AC2EFF) (Fig. 1). A complete set of time series plots are included as supplemental figures using log concentration axes to better present low concentration data (Figs. S-1 to S-6). Cumulative probability data for metal concentrations are contained in supplemental

Figs. S7–S12. The project treatment goals (discussed in Sobolewski et al. 2022, this issue) are presented in Table 3 and Figs. 5, 6, 7, 8, 9, 10 and are primarily dissolved metals standards. However, for discharge permits in Colorado, effluent monitoring to determine compliance with metals must use the “potentially dissolved” method unless it is demonstrated that the dissolved analyses are statistically comparable to the potentially dissolved analysis (CDPHE 2017). For this study, total recoverable metals were used as a conservative surrogate for potentially dissolved concentrations and were compared with project treatment goals, along with dissolved concentrations.

The behavior of metals in the VBTT water depended on whether each metal was dominated by adsorbed/precipitated phases (e.g. Fe, Pb, and Cu to some extent), or soluble metals concentrations (e.g. Mn, Cd, and Zn). The seasonal variability of total Fe concentrations in the VBTT influent (Fig. 7) shows that the highest concentrations occurred before and after freshets and correlate to some extent with turbidity. Carryover from the settling basin at SB2 during these shoulder seasons results in filtration of Fe particulates at the surface of the biotreatment cell media (based on visual observation) and is important to the required maintenance and long-term life expectancy of the media. Figures 7, S-3 and the cumulative probability plot for total Fe concentrations (Fig. S-9) at the VBTT effluent show that only one point exceeded the project treatment goals by a small margin.

Total Pb is another metal that is primarily in the solid phases at the VBTT influent and correlates with Fe, suggesting that it is predominately sorbed to Fe oxides (Fig. 9). The highest concentrations were in the freshet's shoulder seasons. The time series plot and cumulative probability plots for total Pb in VBTT effluent (Figs. S-5 and S-11) illustrate that Pb met all project treatment goals during the study (Table 4).

Total Cu shows mixed behavior, being predominantly sorbed to Fe oxides during the freshet shoulder seasons, but with higher dissolved concentrations during the lower pH freshet periods (Fig. 6). The dissolved Cu carries through the settling basin (SB2) but is attenuated readily in the biocell (BTEFF) by complexation to organic matter and sulfide precipitation. The time series plots and cumulative probability plot for total Cu (Figs. 6, S-2, and S-8) show that total Cu met project treatment goals throughout the study on both a total and dissolved basis (Table 4).

Zn primarily entered the VBTT in the soluble phase and total Zn concentrations (Fig. 10) reached their highest influent concentrations immediately as the mine drainage hydrograph began to rise (Lewis-Russ et al. 2022). Changes in influent pH are subtle during freshet (minimum values of 6.5–6.2 compared to 6.8–7.1 during non-freshet periods) but these corresponding increases in dissolved Zn concentrations during freshet are consistent with smithsonite

Table 1 Summary of influent water chemistry (Median values) from the St Louis Tunnel

Analyte	Units	Median values		Freshet max/min	
		Total analysis	Dissolved analysis	Total freshet	Dissolved freshet
Al	µg/L	726	86.3	2070	1780
As	µg/L	<0.065	<0.065		
Cd	µg/L	22	21.2	88.5	88.2
Cu	µg/L	129	14.3	777	690
Fe	µg/L	5730	2020		
Pb	µg/L	4.4	<0.13		
Mn	µg/L	2290	2260	4310	4260
Ni	µg/L	5.5	5.5	11.1	11.0
Zn	µg/L	4070	3850	14,700	14,400
pH	su		6.7		6.2 (min)
ORP	mV (Ag/AgCl)		27		163
Alkalinity	mg/L		97.4		32 (min)
Sulfate	mg/L		622		908

Values are highly seasonal and extreme values during freshet are included if they occur (Lewis-Russ et al. 2022). Values during freshet are maxima, except where noted

Fig. 2 Field pH data. Primary sampling locations include Mine Water Influent, Settling Basin 2 Effluent (SB2EFF), Biotreatment Cell Effluent (BTEFF), and Aeration Cascade Effluent (AC2EFF). Note: Spring freshets indicated by blue shaded bars

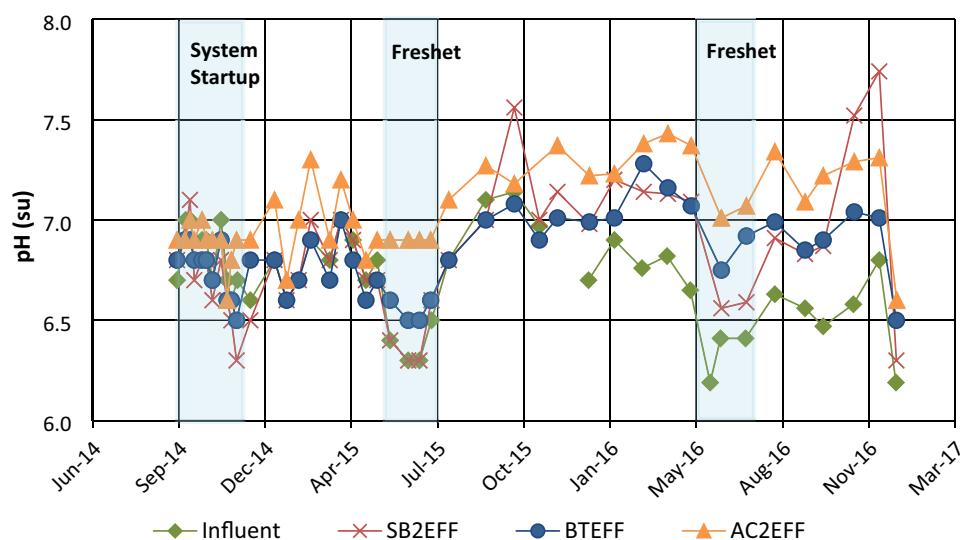
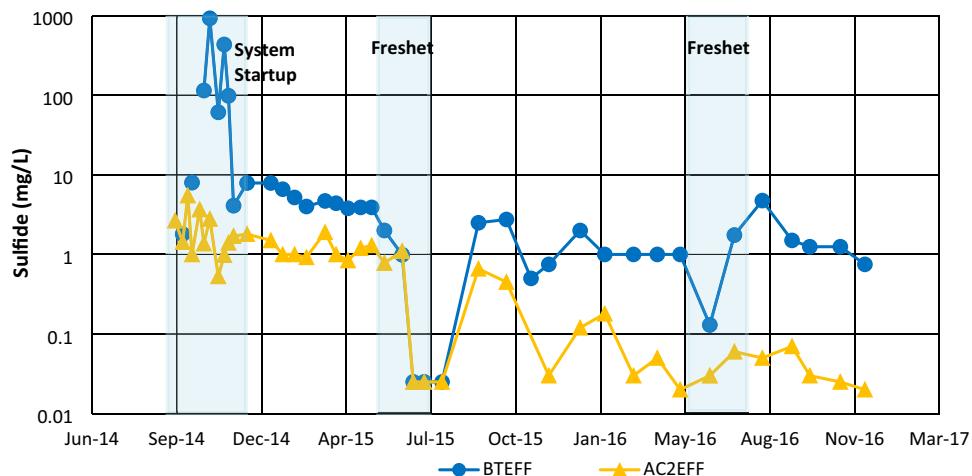


Fig. 3 Sulfide concentrations in the biocell effluent (BTEFF) and Aeration cascade (AC2EFF) plotted as a function of time. Note freshet seasons denoted by blue shaded bars. Data < DL were plotted as ½ DL



equilibrium (Lewis-Russ et al. 2022, this issue). There was limited attenuation as Fe precipitated in the settling basin, but most of the Zn passed through the settling basin (SB2) and into the biocell. The Zn concentrations exceeded the treatment capacity of the biocell and cascade aerator (AC2), and total concentrations exceeded the project goals during the freshet seasons of 2015 and 2016 (Figs. 10, S-6). The cumulative plot for total Zn indicates that project treatment goals were met 49% of the time (dissolved 95%), more frequently following system startup (61%), and frequency increased to the end of the study (Table 4 and Fig. S-12). Plots for total Cd concentrations and cumulative probability are shown in Figs. 5 and 11, respectively. Total Cd

concentrations of the VBTT effluent were within project treatment goals throughout the study (Table 4).

Manganese is also predominantly soluble in the VBTT influent and shows similar behaviors to Zn, with influent Mn concentrations during freshet consistent with rhodochroite equilibrium (Lewis-Russ et al. 2022). Exceedances of project treatment goals occurred during system start up and freshet seasons (Fig. 8). Although significant attenuation of Mn in the VBTT was not expected, significant Mn attenuation occurred in both the biocell and aeration cascade (AC2). The cumulative probability plot for total Mn illustrates that 80% met project treatment goals (95% for dissolved),

Fig. 4 Average monthly temperature for water within the Vertical Wetlands Treatment Train (VWTT) at the Influent and effluents of the Settling Basin (SB2EFF), Biotreatment Cell Effluent (BTEFF), and Aeration Cascade (AC2EFF). Locations in Fig. 1

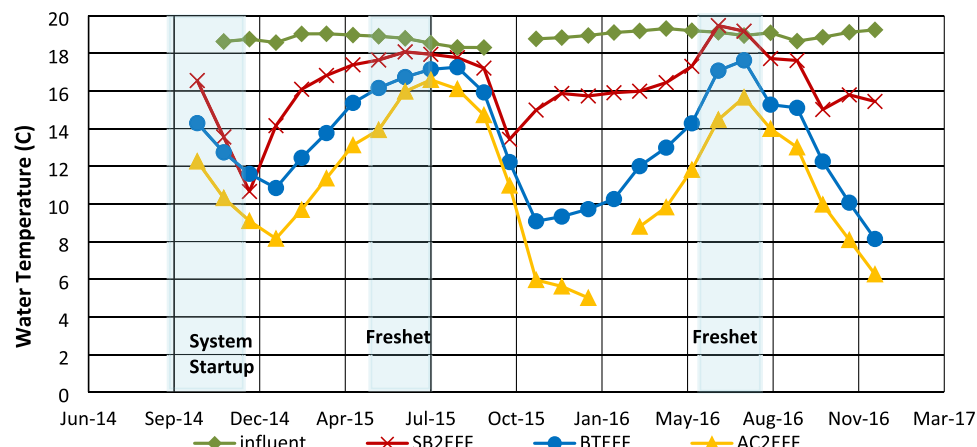


Table 2 Percent increase in metals concentration during spring freshet—Cd, Cu, Mn, and Zn

	Cd (T) %	Cd (D) %	Cu (T) %	Cu (D) %	Mn (T) %	Mn (D) %	Zn (T) %	Zn (D) %
2015 Freshet increase	298	318	251	246	129	123	256	284
2016 Freshet increase	361	441	870	95.6	92.9	102	280	283

The “T” and “D” refer to total and dissolved sampling/analytical methods and data, respectively

Fig. 5 Total cadmium data. Primary sampling locations include Mine Water Influent, Settling Basin 2 Effluent (SB2EFF), Biotreatment Cell Effluent (BTEFF), and Aeration Cascade Effluent (AC2EFF). Note: Spring freshets and system startup indicated by blue shaded bars

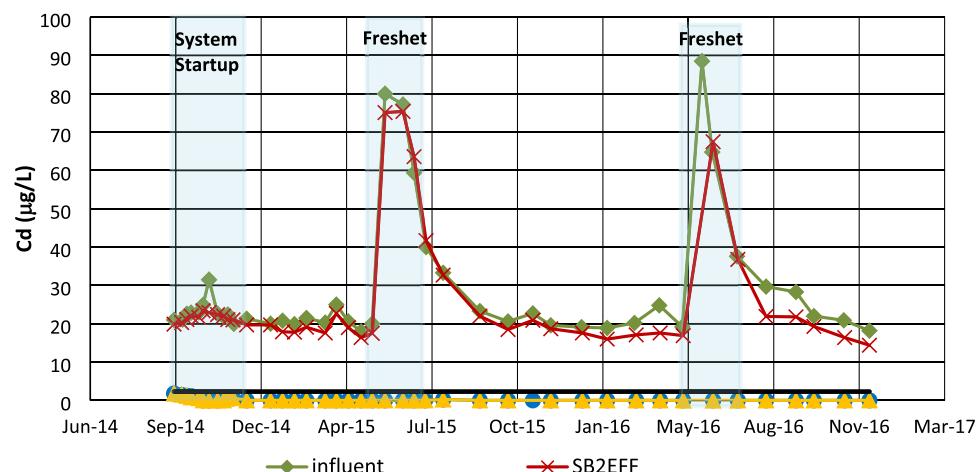


Fig. 6 Total copper data. Primary sampling locations include Mine Water Influent, Settling Basin 2 Effluent (SB2EFF), Biotreatment Cell Effluent (BTEFF), and Aeration Cascade Effluent (AC2EFF). Note: Spring freshets and system startup are indicated by blue shaded bars

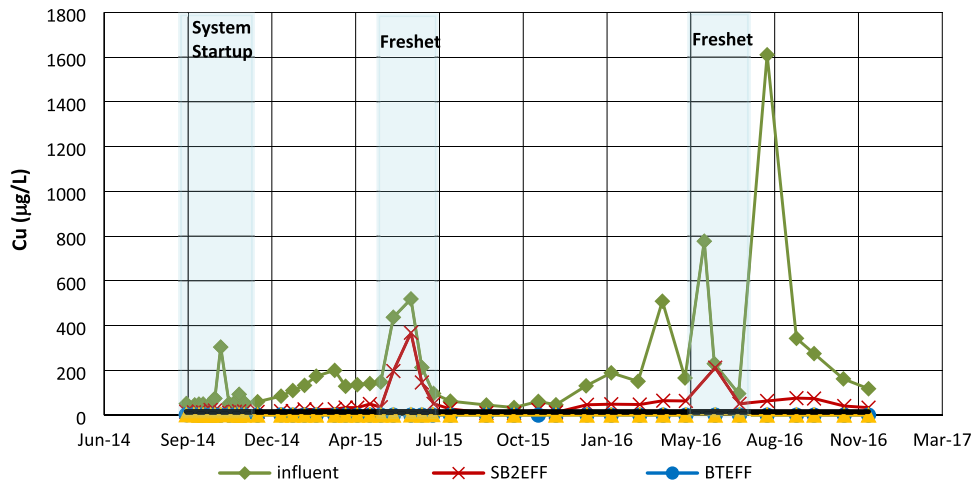


Fig. 7 Total iron data. Primary sampling locations include Mine Water Influent, Settling Basin 2 Effluent (SB2EFF), Biotreatment Cell Effluent (BTEFF), and Aeration Cascade Effluent (AC2EFF). Note: Spring freshets and system startup are indicated by blue shaded bars

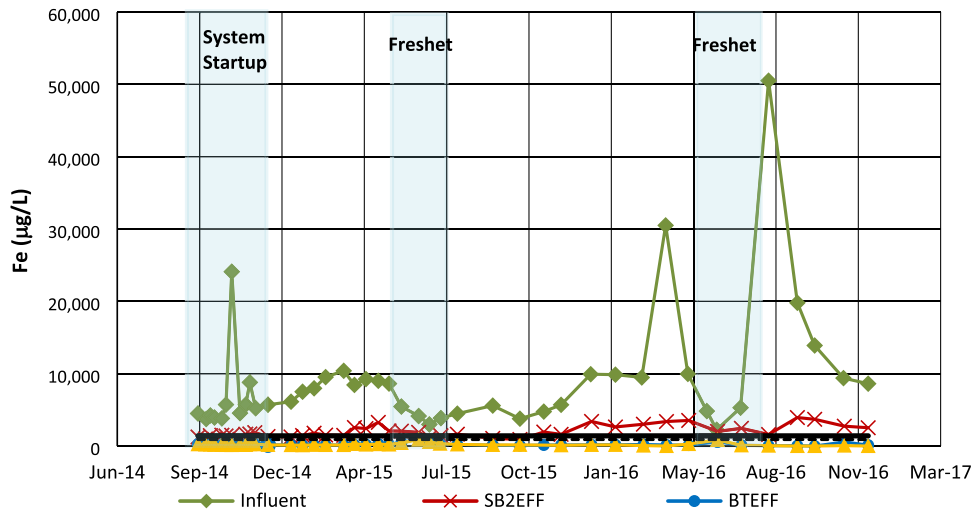


Fig. 8 Total manganese data. Primary sampling locations include Mine Water Influent, Settling Basin 2 Effluent (SB2EFF), Biotreatment Cell Effluent (BTEFF), and Aeration Cascade Effluent (AC2EFF). Note: Spring freshets and system startup are indicated by blue shaded bars

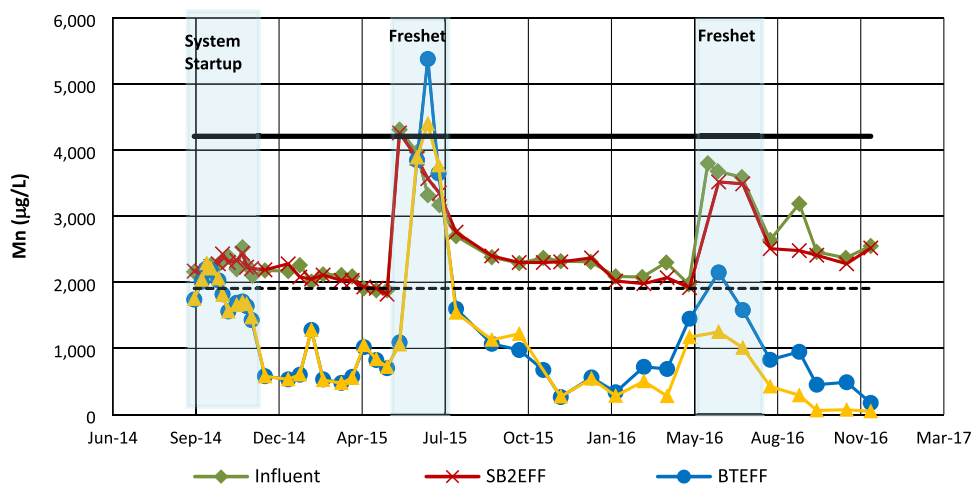


Fig. 9 Total Lead Data. Primary sampling locations include Mine Water Influent, Settling Basin 2 Effluent (SB2EFF), Biotreatment Cell Effluent (BTEFF), and Aeration Cascade Effluent (AC2EFF). Note: Spring freshets and system startup are indicated by blue shaded bars

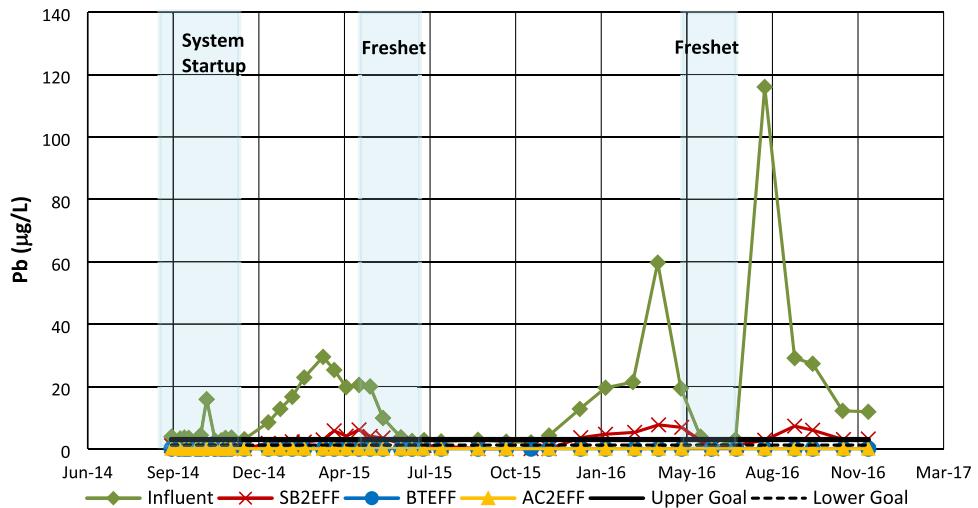


Fig. 10 Total zinc data. Primary sampling locations include Mine Water Influent, Settling Basin 2 Effluent (SB2EFF), Biotreatment Cell Effluent (BTEFF), and Aeration Cascade Effluent (AC2EFF). Note: Spring freshets and system startup are indicated by blue shaded bars

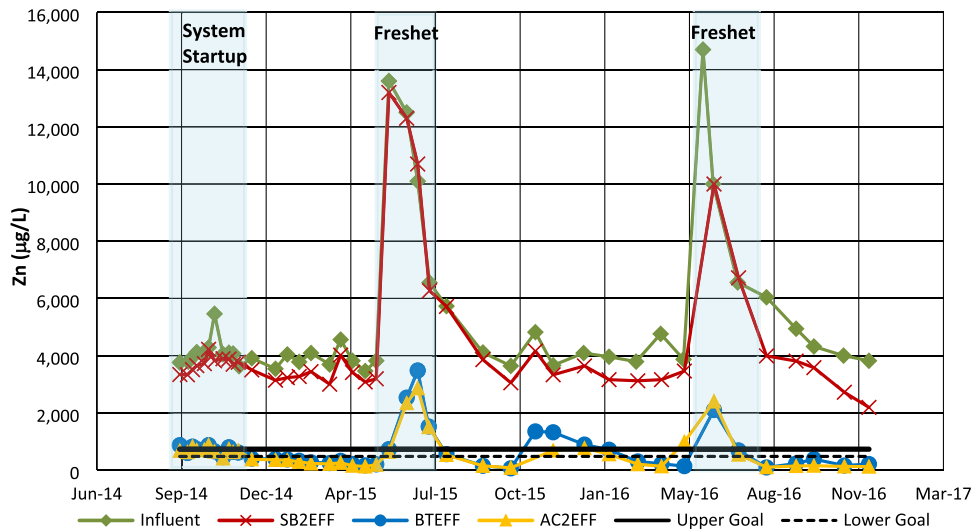


Table 3 Project treatment goals for performance evaluation of the Vertical Wetlands Treatment System

	As, T µg/L	Cd, D µg/L	Cu, D µg/L	Fe, T µg/L	Pb, D µg/L	Mn, D µg/L	Ni, D µg/L	Zn, D µg/L
Lower target	ND	2.3	8.1	903	1.22	1,908	10	476
Upper target	3.7	2.3	15.7	1,410	3.00	4,210	48	729

The “T” and “D” refer to total and dissolve sampling/analytical techniques and data, respectively

more frequently (90%) as the system matured (Fig. S10, Table 4).

Discussion

The time series plots (Fig. 2 through Fig. 10) illustrate dramatic seasonal variation in influent metals concentrations, pH, and sulfide concentrations during the “freshet” period from mid-May to mid-July (Lewis-Russ et al. 2022). The form of these metals (particulate vs. soluble) determines the mechanisms of attenuation and the difficulty of treatment. The above results illustrate that Fe, Pb, and Cu were primarily particulate, removed for the most part in the settling basin, have high removal efficiencies (Table 4), and met project treatment goals over the course of the study. Cd behaved similarly to Zn, but total and dissolved Cd were below project treatment goals throughout the study. The remaining discussion will be limited to Mn and Zn, which occur in the influent as dissolved species and were the greatest challenge.

Zinc Attenuation

Meeting project treatment goals for Zn was problematic with 49% and 95% of concentrations meeting goals for total and dissolved Zn concentrations, respectively (Table 4 and Figs. 10 and S-6). Attenuation of total Zn in the system predominately occurred in the biocell and is best followed as the difference between the biocell influent (SB2EFF) and effluent (BTEFF) in Fig. 11. Total and dissolved Zn were attenuated in the biocell as ZnS precipitated, with an 88.6% and 98.2% average removal efficiency, respectively (Table 4). Comparison of influent vs. effluent total Zn concentrations illustrates that high levels of attenuation were

operable from the initiation of the VBTT and also illustrates that most of the Zn discharged from the biocell was particulate ZnS. The average Zn concentrations in the total suspended solids from the BTEFF during both freshet seasons are estimated at 57% and 85% (respectively) on a ZnS basis ($(Zn_{Tot} - Zn_{Diss})/TSS$). Scanning electron microscopy with energy dispersive x-ray spectroscopy (SEM-EDX) was used to image and analyze $> 0.45\text{-}\mu\text{m}$ filter residue collected from effluent water at BTEFF. The SEM micrograph presented in Fig. 12 illustrates that the filter residue material was a fine-grained filter cake, with particle sizes typically below resolution (e.g. $< 1\text{ }\mu\text{m}$). The SEM-EDX spectra also illustrates that the material was predominantly ZnS (78% by weight). Colloidal ZnS particles have been noted in wetlands literature and this likely explains the ability of some of the ZnS particulates to pass through the filtering capabilities of the biocell (Gammons and Frandsen 2001; Jarvis et al. 2015).

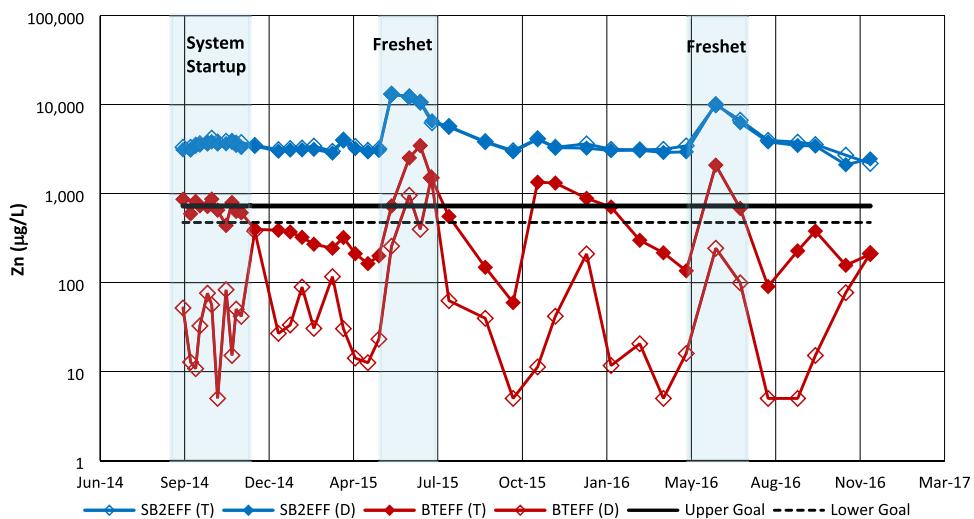
The highest concentrations of total and dissolved Zn in the settling basin (SB2EFF) and biotreatment cell (BTEFF) effluents occurred during the 2015 freshet (Fig. 11), when pH and sulfide concentrations in the biocell were low (Figs. 2 and 3). Since sulfide concentrations went below detection during that time, there was speculation that the SRB were functioning at a diminished level during that season. A mass balance for Zn and residual dissolved sulfide described by Sobolewski et al. (2022) is included as Fig. 13. The total precipitation capacity (TPC) is the sum of the $\mu\text{mol/L}$ of Zn precipitated as ZnS and residual sulfide discharged from the BTEFF. Figure 13 contains a time series accounting of the precipitated calculated TPC and ZnS across the BT cell, total and dissolved Zn concentrations at BTEFF, dissolved Zn at BTINF, and the lower TPG. The startup of the VBTT resulted in high levels of dissolved organic carbon that resulted in very high concentrations of sulfides over the

Table 4 Frequency table for meeting project treatment goals for total and dissolved metals concentrations at the effluent of the VWTT system

Analyte	Percentage meeting project treatment goals (%)					
	All evaluation samples (n=41)		Post startup samples (n=31)		Average monthly removal percentage (n=41)	
	Total	Dissolved	Total	Dissolved	Total	Dissolved
As	100	100	100	100	NA	NA
Cd	100	100	100	100	99.1	99.9
Cu	100	100	100	100	99.4	99.5
Fe	98	100	97	100	95.9	82.5
Mn	83	83	90	90	49.6	50.7
Ni	100	100	100	100	NA	NA
Pb	100	100	100	100	NA	NA
Zn	49	95	61	94	88.6	98.2

Also includes average monthly removal rates. Less than detection data calculated with $\frac{1}{2}$ MDL. The NA indicates that the average removal percentage was not calculated because the majority of data were below detection limits

Fig. 11 Total (T) and dissolved (D) Zn concentrations plotted over time for influent (SB2EFF) and effluent (BTEFF) water for the anaerobic biocell. Note: blue shaded bars denote freshet seasons for 2015 and 2016. Less than detection data plotted as $\frac{1}{2}$ MDL



first two months, exceeding the amount required for metal attenuation. A steadily declining TPC occurred following startup until initiation of the 2015 freshet, when the amount of Zn (D) in the influent and Zn attenuation increased greatly and the residual sulfide decreased during the first two dates and went to < DL during the next three dates. Dissolved Zn broke through the lower TPG at BTEFF on two dates during the 2015 freshet; however, total Zn containing ZnS particulates occurred at higher concentrations and broke through at all freshet dates. Although the TPC declined through the 2015 freshet (plus one additional sampling date), there was still significant Zn attenuation, implying that SRB activity was only partially inhibited, or sulfide accumulated within the biotreatment cell was being mined. The reductions in SRB activity and residual sulfides could have been related to the lower pH (6.2), as the SRBs present from before the freshet were acclimated to the somewhat higher pre-freshet

pH. A lower pH could be affecting the growth or sulfate reduction rate in the SRBs or the microbial community that supports them. While acidophilic strains have been isolated from acidic environments, most known SRBs are neutrophilic with an optimal pH range of 6–8 (Sánchez-Andrea et al. 2014). There is evidence to suggest that pre-exposure to unfavorable conditions (e.g. aerobic stress, high metals loading, etc.) could select for more resilient populations of SRB that can be used to inoculate and treat a biocell (Lefèvre et al. 2013). Specific metal inhibition of SRB activity could also contribute to reduced activity. Laboratory studies in bioreactors (Utgikar et al. 2001) have shown EC50 values (minimum concentration to cause 50% reduction in sulfate reduction) of 14 mg/L for Zn, consistent with influent Zn concentrations during freshet experienced in our field study (Fig. 10). Additional studies have shown that solid-phase metal sulfides can reduce SRB activity in

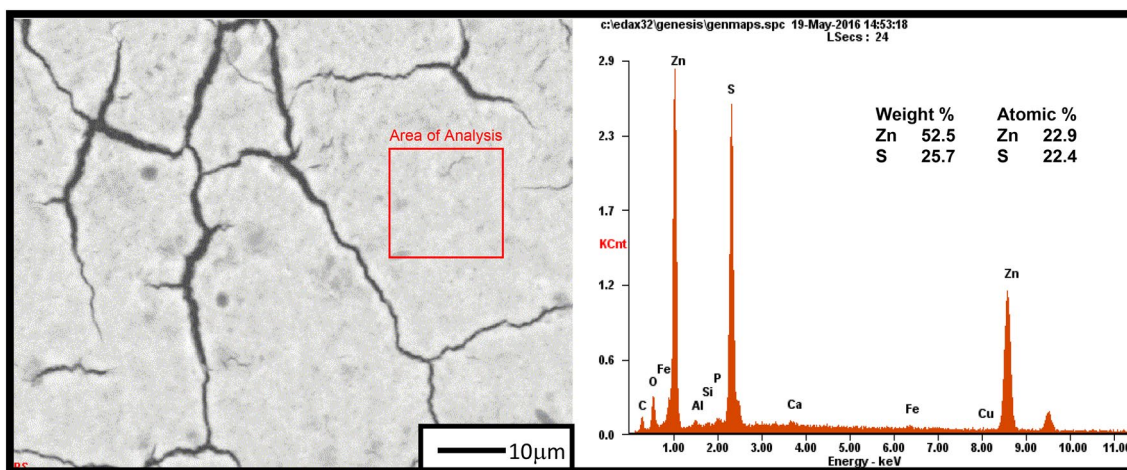


Fig. 12 SEM Micrograph and Elemental Analysis of Biocell Effluent (BTEFF) Filter Residue (0.45 µm filter). Individual particle size in the filter cake is below resolution of the SEM and likely less than 1 µm

laboratory cultures by coating SRB cells with sulfide crystals, as opposed to specific metal toxicity (Utgikar et al. 2002). The TPC resumed the same steady post-startup rate of decline following the 2015 freshet (Fig. 13). During the fall and winter of 2015/2016, total Zn exceeded the lower TPG, but there was residual sulfide at BTEFF and exceedances were driven by particulate ZnS. The exceedances of the total Zn TPG in fall/winter 2015/2016 were most likely caused by an operational adjustment made in late October 2015 (increased water level) and were not related to BT cell influent water chemistry. The freshet of 2016 was less severe and the SRBs were likely better acclimated to the abrupt onset of freshet conditions. Residual sulfides were very low on the lowest pH sampling date, but dissolved Zn at BTEFF remained below the lower TPG and particulate ZnS resulted in a slight exceedance of total Zn at both 2016 freshet sampling dates. Carryover of particulate ZnS seems to be as important as diminished SRB activity during the freshet.

Laboratory data from the 2015 freshet lagged some of the field observations and a response to the metals breakthrough was to increase the water level at the outflow of the biocell to increase the hydraulic retention time and the saturated volume of media in the biocell. That learning was used in 2016 when the water levels were proactively raised prior to the freshet, based on the telemetry system data. Less dramatic freshet effects were noted in 2016. Similar behavior was noted, to a lesser extent, for highest total concentrations

of Cd and Cu during freshet conditions; however, these all met project treatment goals (Figs. 5 and 6).

Manganese Attenuation

Manganese removal observed in the biocell was unexpectedly high, with an average removal efficiency of 50% and a maximum removal efficiency of 98% (Table 4, Fig. 14). Manganese removal rates in sulfate-reducing bioreactors are typically low (Brookens et al. 2000; Carty et al. 2001; Watzlaf et al. 2000). Removal as manganese sulfide (MnS) was considered unlikely because Mn does not readily form a stable sulfide under reducing anaerobic conditions (Doshi 2006; Gammons and Frandsen 2001). Preliminary results from an ongoing investigation indicate that Mn is oxidizing from Mn(II) to Mn(IV) in the upper 20 to 30 cm of the biocell matrix and precipitating as Mn oxides. Data from Sobolewski et al. (2022) suggests that Mn is precipitated in the oxidizing transition zone at the leading edge of the bioreactor.

Manganese removal efficiency has been added to Fig. 8 to form Fig. 14 and shows how Mn removal changed during the study. Removal of Mn started at 0% as the readily available organic carbon in the biocell developed low ORP and high sulfides. These high sulfide (low ORP) conditions diminished abruptly in November 2014, when total Mn removal efficiency rose to 75%. After degradation of much of the labile organic carbon, a transition zone in the leading (more

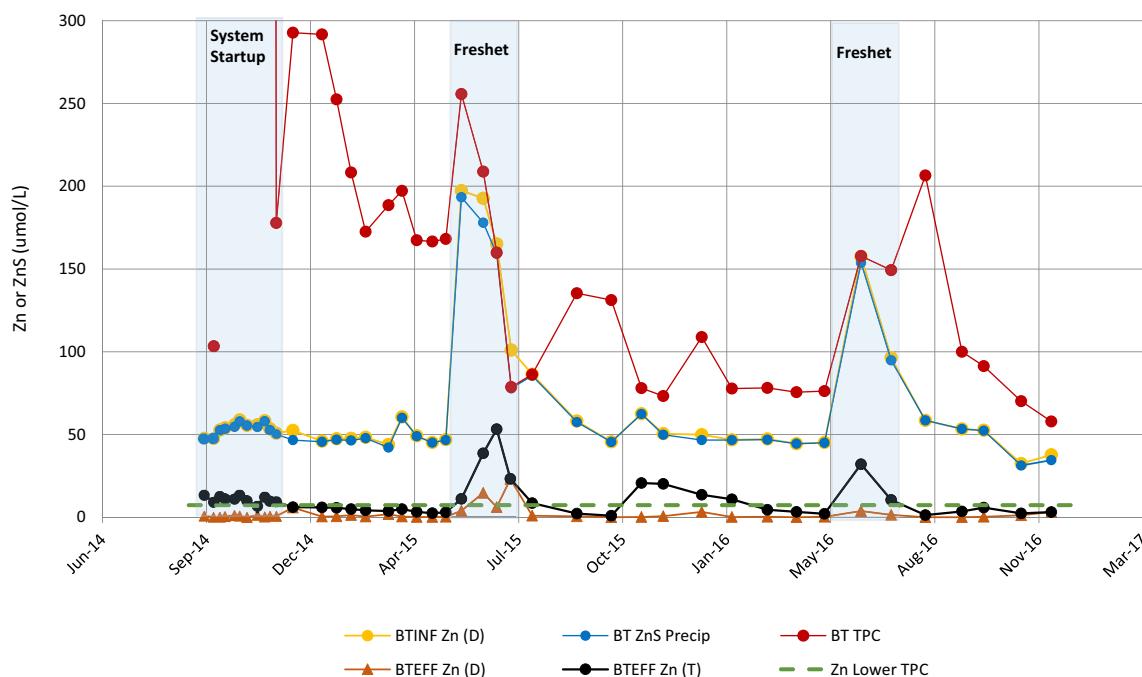


Fig. 13 Time series plot of dissolved Zn at the biocell influent (BTINF) and effluent (BTEFF), total Zn at the BTEFF, ZnS precipitated and total precipitation capacity (TPC) across the BT cell. <DL concentrations calculated and plotted as $\frac{1}{2}$ MDL

oxidized) portion of the biocell appears to have provided an environment conducive to Mn-oxidizing bacteria where Mn could be oxidized and precipitated (Sobolewski et al. 2022). The freshet initiation of 2015 had a severe impact on Mn removal (Fig. 14), likely due to the lower pH and/or increased dissolved metals concentrations on the activity of Mn-oxidizing bacteria. Negative effects on Mn removal were greater than other metals in the study. Manganese may have been temporarily remobilized from part of the biocell during the 2015 freshet, where peak concentrations of total and dissolved Mn in the BTEFF and AC2EFF occurred one month following the peak influent concentrations (Fig. 14). The later peak that eluted at BTEFF and AC2EFF contained higher concentrations of total and dissolved Mn than the peak concentrations at the influent and SB2EFF, resulting in negative removal efficiency values. Lower pH values and slightly higher dissolved Fe concentrations during this period may have contributed to reductive dissolution of previously attenuated Mn. As the effects of the 2015 freshet diminished, Mn removal rates increased to values at or above those seen before the freshet conditions.

Unexpected Mn removal also occurred in the aeration cascade. For the first 17 months of operation, no Mn removal occurred in the aeration cascade (Fig. 14). Starting in March 2016, however, Mn removal was noted in the aeration cascade, with typical removal efficiency values for the VBTT increasing to 85%. Black staining of the rock media in the cascade was consistent with Mn oxidation and precipitation. Residual sulfides in the aeration cascade reached low concentrations at this time and continued to decline to the end of the study (Fig. 3). Mn removal was not anticipated in the aeration cascade as the HRT was less than 30 min, whereas oxic Mn removal systems typically employ HRTs longer than 12 h (Nairn and Hedin 1993). The freshet conditions of 2016 again negatively impacted the Mn removal

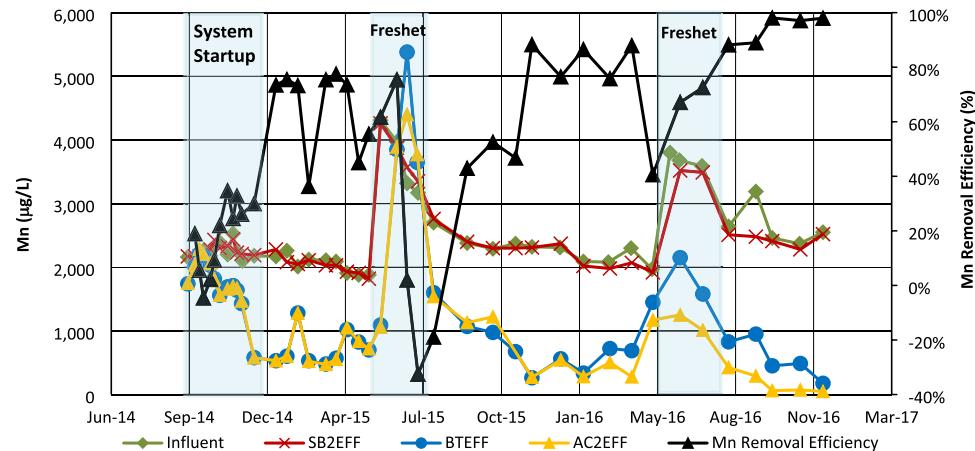
efficiency (to a lesser extent) and removal stayed lower until the effects of the freshet diminished. The system continued to mature and develop Mn removal capacity following the freshet, resulting in 98% removal efficiency at the end of the study (Fig. 14).

System Management

Improved frequency of meeting treatment goals in 2016 is the result of multiple factors related to system management and maturity of the biocell. Following startup of the VBTT in Fall 2014, organic matter in the media was fresh and ORP values as low as -444 mV were observed. Concerned that these conditions might favor methanogenesis, the water level in the biocell was reduced below the maximum to decrease HRT, increasing ORP values. The water level was raised to the maximum level in June 2015 after analytical data indicated biocell metals removal had been negatively impacted by the reduced influent pH and increased metals concentrations. Increasing the HRT and quantity of saturated media in contact with the water improved sulfide generation and system performance. The water level was lowered again in November 2015, causing slight exceedances of total Zn for several months (Fig. 10), and then preemptively raised back to the maximum in April 2016 in anticipation of the freshet. The biocell water level was maintained at its maximum level since that time. Less freshet effects were noted in 2016 and excessively low ORP values were not observed since 2015, due to maturation of the organic media.

The robust nature of the system was demonstrated during 2016, when influent flow to the system was shut off multiple times for periods of two to seven days to accommodate construction activity at the site. Restarting the system consisted of only re-introducing flow, and sampling data indicate that the system was not adversely affected by the shutdowns.

Fig. 14 Time series plot of total Mn over time for each component of the VWTT system from Fig. 11 plotted with Mn removal efficiency (%) to show evolution of the system over time



Conclusions

Overall, data from the study indicate that the VBTT provided effective, reliable treatment of metal-bearing mine drainage at the site. The system is robust and operates with minimal oversight and operational input. Adjustments to water height in the cells were required on startup to prevent excessively low ORP values, but little adjustment was required during the rest of the study. The system was well suited to the site conditions, including: circumneutral mine drainage, geothermal inputs, and limited site access and on-site safety issues during the harsh winters.

Effects of seasonal ambient temperature on system performance were limited by consistent inputs of warm geothermal mine influent waters (18–19 °C) and system design (including below grade construction of ponds and other thermal conservation measures), which may be incorporated into other site settings. Thermal effects were overshadowed by the effects of the spring freshet on the chemistry of the influent waters.

Seasonal fluctuations of influent metal concentrations and pH values presented the greatest challenges to meeting project treatment goals. Monitoring data indicates that future exceedances of project treatment goals for Mn and Zn total concentrations are possible, if not likely, during 6- to 8-week freshet periods of some years. Total Zn concentrations during freshet seasons is the primary limitation to meeting project treatment goals. Most of the total Zn and TSS leaving AC2EFF was colloidal ZnS and represents an opportunity to improve system performance.

Manganese attenuation was significant in both the biocell and aeration cascade due to biochemical oxidation and precipitation of Mn oxides in transition zones. Manganese attenuation occurs year-round at the temperatures within the VBTT.

The telemetry system provided real time data that was used to observe dynamic changes in pH and other parameters. This was used to proactively manage system flow parameters, improve safety, optimize sampling occurrence, and provided measurements equilibrated with parameters such as pH and ORP.

Supplementary Information The online version contains supplementary material available at <https://doi.org/10.1007/s10230-022-00857-8>.

Acknowledgements The authors thank BP for access to the study site and for funding the research.

Open Access This article is licensed under a Creative Commons Attribution 4.0 International License, which permits use, sharing, adaptation, distribution and reproduction in any medium or format, as long as you give appropriate credit to the original author(s) and the source, provide a link to the Creative Commons licence, and indicate if changes were made. The images or other third party material in this article are included in the article's Creative Commons licence, unless indicated

otherwise in a credit line to the material. If material is not included in the article's Creative Commons licence and your intended use is not permitted by statutory regulation or exceeds the permitted use, you will need to obtain permission directly from the copyright holder. To view a copy of this licence, visit <http://creativecommons.org/licenses/by/4.0/>.

References

Brookens AM, Schmidt TW, Branch WL (2000) The effectiveness of utilizing passive treatment systems for leachate discharges in western Maryland. Presented at the American Soc for Surface Mining and Reclamation(ASMR) 17th Annual Meeting

Canty M, Hiebert R, Harrington-Baker MA, Bless D (2001) Innovative, in situ use of sulfate reducing bacteria to remove heavy metals from acid mine drainage. In: Proc, 2001 International Containment and Remediation Technology Conf and Exhibition. doi:10.1.1.549.4790&rep=rep1&type=pdf

CDPHE (Colorado Dept of Public Health and Environment) (2017) Water Quality Control Commission. Regulation No. 31 - The basic standards and methodologies for surface water, 5 CCR 1002–31. December 28, 2020. https://www.colorado.gov/pacific/sites/default/files/31_2017-03.pdf

Doshi SM (2006) Bioremediation of acid mine drainage using sulfate-reducing bacteria. U.S. Environmental Protection Agency, Office of Solid Waste and Emergency Response, Office of Superfund Remediation and Technology Innovation

Figueroa L, Seyler J, Wildeman T (2004) Characterization of organic substrates used for anaerobic bioremediation of mining impacted waters. In: Jarvis A (ed) Proc, International Mine Water Assoc Conf, pp 43–52

Gammons CH, Frandsen AK (2001) Fate and transport of metals in H₂S-rich waters at a treatment wetland. *Geochem Trans*. <https://doi.org/10.1186/1467-4866-2-1>

Gammons CH, Mulholland TP, Frandsen AK (2000) A comparison of filtered vs unfiltered metal concentrations in treatment wetlands. *Mine Water Environ* 19:111–123

Gusek JJ, Wildeman TR, Miller A, Fricke J (1998) The challenges of designing, permitting and building a 1,200 gpm passive bioreactor for metal mine drainage, West Fork Mine, MO. In: 15th Annual Meeting, American Soc of Surface Mining, Reclamation (ASSMR). <https://doi.org/10.21000/JASMR98010203>

Hagerty P, Figueroa L, Fricke J (2011) The effect of substrate particle size on sulfate reduction treatment efficiency of mining influenced water. Soc of Mining Metallurgy and Exploration (SME) Annual Meeting, Denver, CO

Hedin RS, Nairn RW, Kleinmann RLP (1994) Passive treatment of coal mine drainage, USDI Bureau of Mines IC 9389, Pittsburgh

Huntsman BE, Solch JB, Porter MD (1978) Utilization of a sphagnum species dominated bog for coal acid mine drainage abatement. Abstracts, 91st Annual Meeting Geologic Soc America, 10(7): 426

Jarvis A, Gandy C, Bailey M, Davis J, Orme P, Malley J, Potter H, Moorhouse A (2015) Metal removal and secondary contamination in a passive metal mine drainage treatment system. In: Proceedings 10th international conference on acid rock drainage (ICARD) and IMWA annual conference, April 21–24, Santiago, Chile

Johnson DB, Hallberg KB (2002) Pitfalls of passive mine water treatment. *Rev Environ Sci Biotechnol* 1:335–343

Kleinmann, RLP (1991) Biological treatment of mine water—an overview. In: Proc, 2nd ICARD, pp 27–42

Lefèvre E, Pereyra LP, Hiibel SR, Perrault EM, De Long SK, Reardon KF, Pruden A (2013) Molecular assessment of the sensitivity of sulfate-reducing microbial communities remediating mine drainage to aerobic stress. *Water Res* 47(14):5316–5325

Lewis-Russ A, Riese AC, Moore TJ, Brown AR (2022) Passive treatment of circumneutral mine drainage from the St Louis Mine Tunnel, Rico CO: part 1—case study: characteristics of the mine drainage. *Mine Water Environ* 41, in this issue

Luther GW III, Findlay AJ, MacDonald DJ, Owings SM, Hanson TE, Beinart RA, Girguis PR (2011) Thermodynamics and kinetics of sulfide oxidation by oxygen: a look at inorganically controlled reactions and biologically mediated processes in the environment. *Front Microbiol* 2:62. <https://doi.org/10.3389/fmicb.2011.00062>

Nairn B, Hedin RS (1993) Contaminant removal capabilities of wetlands constructed to treat coal mine drainage. In: Moshiri GA (ed) *Constructed wetlands for water quality improvement*. CRC Press, Boca Raton, pp 187–195

Neculita C, Zagury G, Bussière B (2007) Passive treatment of acid mine drainage in bioreactors using sulphate-reducing bacteria: critical review and research needs. *J Environ Qual* 36:1–16

Postgate JR (1984) *The sulfate-reducing bacteria*, 2nd edn. Cambridge Univ Press, Cambridge

Sánchez-Andrea I, Stams AJM, Hedrich S, Nancuchoe I, Johnson DB (2014) *Desulfosporosinus acididurans* sp. nov.: an acidophilic sulfate-reducing bacterium isolated from acidic sediments. *Extremophiles* 19:39–47

Sobolewski A, Riese AC, Moore TJ, and Brown AR (2022) Passive treatment of circumneutral mine drainage from the St Louis Mine Tunnel, Rico CO: part 3—horizontal wetlands treatment train pilot study. *Mine Water Environ* 41, in this issue

TU Delft (2010) Aeration and gas stripping. Delft Univ of Technology OpenCourseWare, January 2010

U.S. EPA (1994) Method 200.8: Determination of trace elements in waters and wastes by inductively coupled-mass spectroscopy. Revision 5.4, U.S. EPA, Cincinnati

Utgikar VP, Chen BY, Chaudhary N, Tabak HH, Haines JR (2001) Acute toxicity of heavy metals to acetate-utilizing mixed cultures of sulfate-reducing bacteria: EC50 and EC100. *Environ Toxicol Chem* 20(12):2662–2669

Utgikar VP, Harmon SM, Chaudhary N, Tabak HH, Govind R, Haines JR (2002) Inhibition of sulfate-reducing bacteria by metals sulfide formation in bioremediation of acid mine drainage. *Environ Toxicol* 17(1):40–48

Watzlaf GR, Schroeder KT, Kairies C (2000) Long-term performance of alkalinity-producing passive systems for the treatment of mine drainage. Presented at the American Society for Surface Mining and Reclamation 17th Annual Meeting. <https://doi.org/10.21000/JASMR00010262>

Widdel F (1988) Microbiology and ecology of sulfate- and sulfur-reducing bacteria. In: Zehnder AKB (ed) *Biology of anaerobic microorganisms*. John Wiley & Sons, New York, pp 469–586

Wieder RK, Lang GE (1982) Modification of acid mine drainage in a freshwater wetland. In: Behling RE (ed) *Proc, Symp on Wetlands of the Unglaciated Appalachian region*. West Virginia Univ Press, pp 43–53